論文 89-26-12-16

Incoherent Optical Signal Processor Using an Acousto-Optic Modulator and a Scanner

(어쿠스토옵틱 광변조기와 스캐너를 사용한 인코히어런트 광신호 처리기)

朴 鎭 雨*

(Jin Woo Park)

要 約

헤테로다이닝을 위한 시간적 오프셋 주파수를 어쿠스토-옵틱 변조기로써 발생시키고 처리 대상체를 주사모드로 처리하고자 광스캐너를 사용한 유용한 인코히어런트 광신호 처리 시스템을 제시하고 분석하였다. 제시된 시스템의 동작특성은 공간필터링에 대하여 광원의 파장폭 변화, 시간적 오프셋 주파수, 그리고 주사속도의 함수로 나타내었다. 또한 시스템의 기능을 높이기 위하여 두가지 OTF 튜닝 방법을 제시하고, MTF 측정과 컴퓨터 계산 결과로써 유효성을 증명하였다.

Abstract

A versatile incoherent optical processing system is developed and analyzed in detail, in which an acousto-optic modulator is used to generate the temporal offset frequency for heterodyning and an optical scanner to process the input object in scanning mode. The operational characteristics of the systems are studied with respect to spatial filtering in terms of the spectral width change of the light source, the temporal offset frequency, and a scanning rate. To enhance the system's capability, two schemes for tuning the system's OTF, structural tuning and defocused object tuning, are also developed and verified with the MTF measurements and computer calculations.

I. Introduction

Optical signal processing has received considerable attention in many areas of applied technology [1,2]. It is due to its advantages of two dimensionality, full processing parallelism, and instantaneous Fourier transform and convolution.

There are two distinct diffraction-based optical information processing schemes; coherent optical processing and incoherent optical processing. Coherent optical processing has received more attention with the advent of the laser source and invention of holograph . Since a coherent system is linear in wave amplitude, it is simple in its

*正會員, 高麗大學校 電子電算工學科
(Dept. of Elec. & Com. Eng., Korea Univ.)

接受日字 : 1989年 5月 22日
(※ 본 연구는 89년도 한국과학재단 연구비 지원으로 행하여 졌음.)

conception and implementation[3]. However, the coherent noise problem from interference between the desired output light distribution and the scattered or reflected light distribution is unavoidable, often leading to unsatisfatory results[4]. Due to such a problem,. incoherent optical processing has been the object of increased research efforts since the seventies. The advantages of incoherent over coherent optical processing are a large system redundancy, insensitivity to object phase characteristics, and a large position tolerence for the filter transparency[5,6]. A conventional incoherent processing system is however seriously limited by the fact that the system is linear in intensity and therefore only non-negative real point spread functions (PSFs) can be implemented, precluding the direct realization of the important operations which requires bipolar PSFs, such as deblurring, differentiation, edge enhancement, etc.

This paper includes in the first part a brief description of a diffraction-based conventional incoherent processing scheme defining its inherent limitation in functionality, and a two-pupil bipolar incoherent processing scheme[7]. Then a more practical incoherent optical processing system utilizing an acousto-optic modulator (AOM) and an optical scanner to form a heterodyne processing configuration is introduced and analyzed in detail. Included are also analyses on the operational characteristics of the system and tunability of the optical transfer function (OTF) of the optical system presented, with experimental verification.

II. Incoherent Optical Processing

1. Coventional Incoherent Processing

In an incoherent system, the representative physical quantity is the real and positive-valued wave intensity distribution. Since the system operates as a linear mapper of intensity, the point spread function (PSF) is proportional to the squared modulus of the coherent amplitude impulse response[3]. A typical incoherent image system is shown in Fig.1, where the object is illuminated by a quasi-monochromatic spatially incoherent light source. The image plane intensity distribution, $I_i(x,y)$ is given by the two-dimensional (2-D) convolutional integral

$$I_i(x,y) = K\iint_{-\infty}^{\infty} h_i(x-\zeta, y-\eta)\, I_o(\zeta,\eta)\, d\zeta\, d\eta, \quad (1)$$

where $I_O(x,y)$ is the object intensity distribution, and $h_i(x,y)$ is the PSF, which is given by

$$h_i(x,y) = |P(x,y)|^2 \quad (2)$$

where P(x,y) being the coherent impulse response which has the relationship with the pupil function p(u,v) of Fig. 1 as

$$P(x,y) = \iint_{-\infty}^{\infty} p(u,v)\, e^{-j2\pi(xu+yv)/\lambda f}\, du\, dv, \quad (3)$$

The constant K is a proportionality factor dependent upon the light transmittance characteristics of the system and of the object, λ the wavelength of the light, f the focal length of the lens. As seen in Eq. (2), the PSF of the conventional incoherent system is always real and non-negative, and as a consequence the OTF of the system has lowpass characteristics posing a inherent limitation. Therefore, a spatial filter which requires zero-amplitude response in the low frequency range can not be realized.

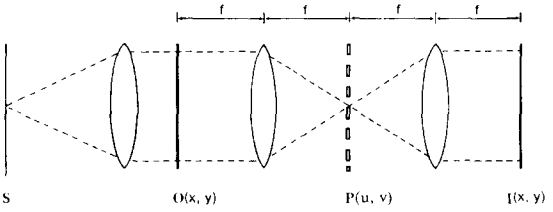

Fig.1. Conventional incoherent imaging system: O denotes the object image plane, I the output image plane, P the pupil plane, and S a spatially incoherent light source.

2. Bipolar Incoherent Processing

A generic diffraction-based incoherent system is shown in Fig. 2, which is a bipolar PSF-generating system based on the work of Lohman and Rhodes[7], and provides a general reference for the incoherence bipolar system.

For this section, the analysis and discussion are carried out in one-dimensional (1-D) unless otherwise stated.

In the imaging system shown in Fig.2 where a spatially incoherent light source illuminates the object 0, the effective pupil function $p_{eff}(\eta)$ is given by the sum of the two transmittance functions

$$p_{eff}(\eta) = A_1 p_1(\eta) e^{j\varphi} + A_2 p_2(\eta), \quad (4)$$

where $p_1(\eta)$ and $p_2(\eta)$ are the pupil functios, A_1 and A_2 the constant transmittance of the two attenuators respectively, and φ is the phase change introduced by the phase shifter. The function variable η is a coordinate variable scaled by $1/\lambda f$. The resulting system transfer function is

$$H_{eff}(\eta) = A_1^2[p_1(\eta) \bigstar p_1(\eta)] + A_2^2[p_2(\eta) \bigstar p_2(\eta)] + A_1A_2[p_1(\eta) \bigstar p_2(\eta)]e^{j\varphi} + A_1A_2[p_2(\eta) \bigstar p_1(\eta)]e^{-j\varphi} \quad (5)$$

where ★ denotes a correlation. Therefore, the corresponding PSF is

$$h_{eff}(x) = A_1^2 |P_1(x)|^2 + A_2^2 |P_2(x)|^2 + A_1A_2P_1(x)P_2^*(x)e^{j\varphi} + A_1A_2P_1^*(x)P_2(x)e^{-j\varphi}. \quad (6)$$

Three different PSF synthesis regimes can be distinguished based on the combination of the terms in Eq.(6): 1) the pupil non-interaction regime, 2) the pupil interaction regime, and 3) the combined regime. The most feasible scheme in synthesizing an arbitrary PSF is the pupil interaction regime, which is resulted from the interference of the two wave distributions originated from the two pupil functions. If the temporal carrier modulation method is to be employed in order to implement a complete processing system, the phase φ can be time-varied and then the PSF information is carried on a temporal modulation frequency of the phase φ. Assuming the phase φ is linearly time-varing, i.e.,

$$\varphi(t) = \alpha t, \quad (7)$$

were α is a constant. The resulting OTF is

$$H_{tem}(\eta) = A_1^2 p_1(\eta) \bigstar p_1(\eta) + A_2^2 p_2(\eta) \bigstar p_2(\eta) + A_1A_2 p_1(\eta) \bigstar p_2(\eta) e^{j\alpha t} + A_1A_2 p_2(\eta) \bigstar p_1(\eta) e^{-j\alpha t}. \quad (8)$$

and the corresponding PSF is

$$h_{tem}(x) = A_1^2 |P_1(x)|^2 + A_2^2 |P_2(x)|^2 + 2A_1A_2 |P_1(x)P_2(x)| \cos[\alpha t + \theta_1(x) + \theta_2(x)] \quad (9)$$

where $\theta_1(x)$ and $\theta_2(x)$ are the spatial phase distributions of P_1 and P_2, respectively. The bipolar PSF term is now carried by the temporal modulation term. The processing output can be extracted by using a non-integrating detector scanning the output. The main limitations of the described two-pupil incoherent system for bipolar PSF synthesis are a large bias background and a system space-bandwidth product limited by the pupil function constraints.

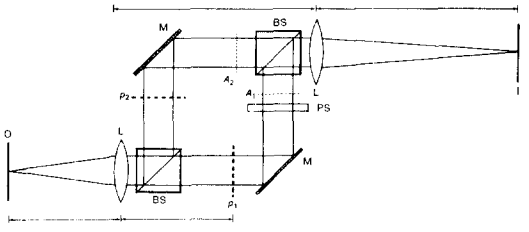

Fig.2. Two-pupil bipolar incoherent system: O denotes the object plane, I the output plane, L the lens, BS the beamsplitter, p_1 and p_2 the pupil functions, M the mirror, PS the phase shifter, and A_1 and A_2 the light attenuators.

III. Acousto-Optic Bipolar Incoherent Processing

1. System Analysis

A realization of the two-pupil incoherent system extended and enhanced from the technique of Poon and Korpel[8] is shown in Fig. 3, which has a Mach-Zehnder interferometer configuration in order to achieve heterodying and an additional functionality, i.e., system tunability. In the system, a wave is amplitude-divided by the first beamsplitter and a frequency offset Δv between the two pupils is introduced by an AOM. After the second beamsplitter, the combined amplitude distribution $g_{com}(x)$ may be written as

$$g_{com}(x) = u(x) + v(x)e^{j2\pi\Delta\nu t}. \quad (10)$$

The field is then imaged onto a mirror mounted on a scanner SC by two identical lenses L_1. The field after the scanner can be written as

$$g_{sc}(x) = [u(x) + v(x)e^{j2\pi\Delta\nu t}] \cdot e^{j2\pi x\, x_{sc}/\lambda f_e} \quad (11)$$

where f_1 is the focal length of the lens L_2, and λ the wavelength of the laser in use. x_{sc} is the scanner's linear motion variable. This variable is defined as a coordinate variable in the x-direction on the object Γ. After Fourier-transforming the amplitude distribution of Eq. (11) by the lens L_2, the resulting distribution on the object plane becomes,

$$G(x_0, x_{sc}) = [U(x_0) + V(x_0)e^{j2\pi\Delta\nu t}] * \delta(x_0 - x_{sc}), \quad (12)$$

where $U(x_0)$ and $V(x_0)$ are the Fourier transforms of $u(x)$ and $v(x)$, respectively, and * denotes convolution. The photodiode PD collects the light after the object and generates the instantaneous current of

$$i(x_{sc}, t) = \int_{-\infty}^{\infty} |G(x_0, x_{sc}) \cdot \Gamma(x_0)|^2 dx_0 \quad (13)$$

Expanding the Eq. (13), the time-varying part, $i_{tv}(x_{sc}, t)$ which has the bipolar information, can be found as in terms of phaser.

$$i_{tv}(x_{sc}, t) = 2\,\mathrm{Re}[I'(x_{sc})e^{-j2\pi\Delta\nu t}], \quad (14)$$

where Re[·] represents the real part of, and the term of our interest is

$$I'(x_{sc}) = [U(-x_{sc})V^*(-x_{sc})] * |\Gamma(x_{sc})|^2. \quad (15)$$

Since an unnormalized OTF is defined as

$$\mathrm{OTF}(f_x) = \frac{\mathrm{FT}\{I'(x_{sc})\}}{\mathrm{FT}\{|\Gamma(x_{sc})|^2\}} \quad (16)$$

where FT denotes the Fourier transform operation, the OTF can be found to be the cross-correlation of the two pupils:

$$\mathrm{OTF}(f_x) = u(\lambda f_1 f_x) \bigstar v(\lambda f_1 f_x) \quad (17)$$

The corresponding PSF is

$$\mathrm{PSF}(x) = U\left(\frac{x}{\lambda f_1}\right) V^*\left(\frac{x}{\lambda f_1}\right) \quad (18)$$

It is noted that the expressions for the OTF and the PSF of the acousto-optic bipolar incoherent system is analogous to the ones of the two-pupil interaction term of the two-pupil incoherent system.

Based on Eq. (17), three examples of OTF synthesis are presented in Fig.4, which represent lowpass filtering and two types of bandpass filtering. Spatial filtering with the two-sided bandpass filter shown in Fig. 4(b) leads to the usual filtering operation, whereas spatial filtering with the one-sided bandpass filter shown in Fig. 4(c) would result in an output in the analytic form[9].

2. System Characteristics

As can be observed in Eqs. (17) and (18), the OTF and the PSF are wavelength-dependent. The OTF and the PSF of a practical system should remain effectively unchanged within a reasonable range of wavelength shifts. Therefore, it is necessary to determine the effect of a spectral shift $\Delta\lambda$. Defining the relative spectral shift as $\gamma = \Delta\lambda/\lambda$, the constraints for the OTF and the PSF can be found in terms of γ. For the OTF, two parameters must be considered: the center frequency of the passband, f_c, and the cutoff

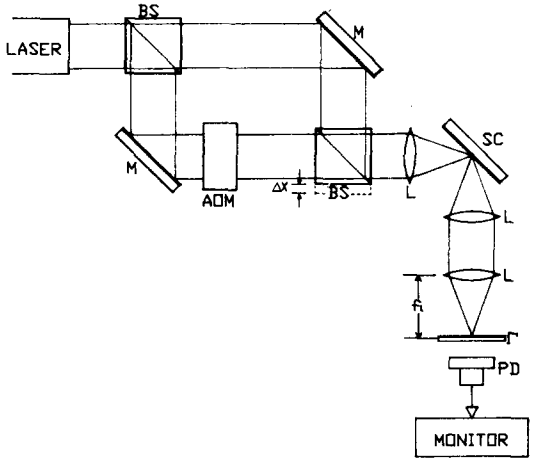

Fig.3. Acousto-optic bipolar incoherent system: BS denotes the beamsplitter, L the lens, M the mirror, AOM the acousto-optic modulator, SC the optical scanner, U and V the pupils, PD the photodetector, and Γ the input object.

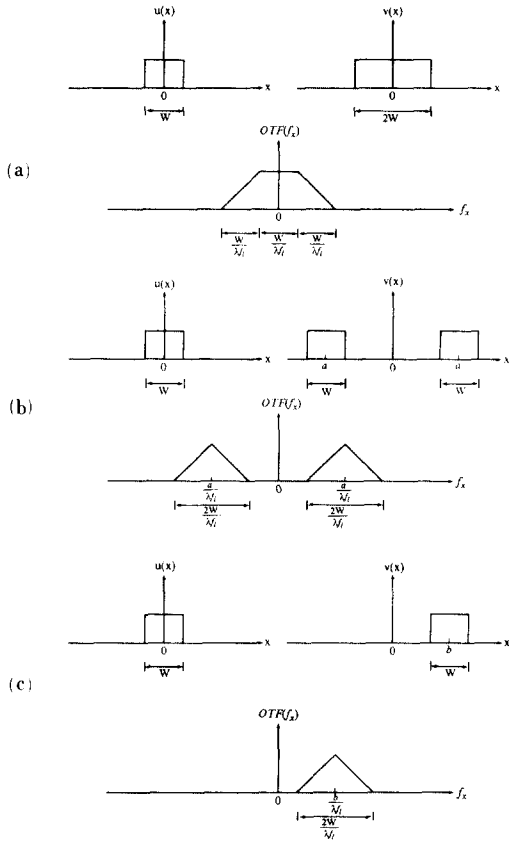

Fig.4. Examples of the OTF synthesis.
(a)a lowpass filter.
(b)a two-sided bandpass filter.
(c)an one-sided bandpass filter.

frequency of the passband, f_o. The relationship between γ and the fractional changes in f_c and f_o is.

$$\frac{\Delta f_c}{f_c}=\frac{\Delta f_o}{f_o}=\frac{\gamma}{1+\gamma} \tag{19}$$

Relating the PSF width to γ, another constraint can be found with respect to the number of the resolution cell of the PSF[5]. Denoting the PSF width as W_p, its fractional change ΔW_p is related to γ by

$$\frac{\Delta W_p}{W_p}=k. \tag{20}$$

If ΔW is require not to exceed the size of a resolution cell of the PSF, the constraint in γ is

$$\gamma<\frac{\alpha}{N}, \tag{21}$$

where N is the total number of the resolution cell within the PSF width W_p, and α is a constant less than 1.0.

In the system shown in Fig. 3, an AOM introduces the temporal frequency offset Δv. This offset frequency Δv must be higher than the maximum frequency of the input signal of interest to avoid aliasing errors near zero frequency. Also, the offset frequency must be large enough to separate the modulated signal from the dc components so as to allow an exact extraction of the output signal. Since the acousto-optic system operates in the scanning mode, the temporal bandwidth of the signal depends on the scanning rate. Assuming that the input image has a spatial resolution of 20 lines/mm, and the scanning rate is 300 Hz within a scanning range of 1 cm, the maximum temporal frequency of the electrical signal on the photodetector is 120KHz. In a practical system, the acousto-optic modulator can easily operate up to 50MHz in the Bragg regime. Consequently, such high offset frequency will satisfy most of the frequency requirements of the processor.

3. OTF Tuning in Acousto-Optic System

In most optical systems, the transfer function can be tuned by adjusting the amplitude transmittance functions of the optical setup. Usually this is done by replacing a photoplate or a mask transparency in the pupil plane. The replacement of such components often requires accurate positioning practice to avoid erroeneous results. Such inefficient and time-consuming practices make tunable optical spatial filtering impractical.

In this section, two methods for tuning the OTF of the acousto-optic incoherent system are investigated and verified experimentally.

1) Structural tuning

From Eq. (17), the OTF is given by the cross-correlation of the two amplitude transmittance pupil funtions. Therefore, a shift of one of the pupils from the axis results in a shift of the OTF. The shift of the puil function in the imaging setup of Fig.3 is obtained by translating the second beam splitter vertically. Taking account of the shift of Δx, the OTF becomes.

$$OTF(f_x) = \int_{-\infty}^{\infty} u(\zeta - \Delta x) v^*(\zeta - \lambda f_i f_x) d\zeta. \quad (22)$$

The advantage of this OTF tuning method is that the chance of perturbing the pupil function position is minimized. This tuning method, however, is applicable only to one-directional operation. In the experiment, two clear pupils were used. Therefore, the amplitude transmittance functions u(x) and v(x) are the same as the amplitude distribution of the laser beam, which is assumed to be Gaussian[10]. Thus, u(x) and v(x) may be written as

$$u(x) = C_1 e^{-(\frac{x}{W_0})^2}, \quad (23)$$

and

$$v(x) = C_2 e^{-(\frac{x}{W_0})^2}, \quad (24)$$

where the amplitude constants C_1 and C_2 are determined by the laser and the beamsplitter used for an amplitude division. W_O is the beam width at 1/e in ampitude. Substituting Eqs. (23) and (24) into Eq. (22), we obtain

$$OTF(f_x) = \exp\left[-\frac{1}{2}\left(\frac{\lambda fe}{Wo}\right)^2\left(fx - \frac{\Delta x}{\lambda fe}\right)^2\right] \quad (25)$$

where an inessential constant factor is ignored for convenience. Note that this OTF is a Gaussian, one-sided bandpass filtering function.

Experimental results of the OTF measurement are given in Fig.5 (a)-(d). The OTFs are estimated with various values of Δx, by scanning a frequency-varying grating object with frequency ranging from 1 line/mm to 20 lines/mm. The curve trace of Fig.5 displayed on the oscilloscope are the responses of the modulation transfer function (MTF), which is the modulus of the OTF. They clearly show that the passband of the MTF moves to the higher frequency range as Δx increases. The center frequency f_c of the passband, where the maximum response occurs, is in good agreement with the theoretical predictions of Eq. (22).

2) Defocused object tuning

The relationship in Eq. (17) is valid only when the object Γ is precisely located at the focal plane of lens L_2. In this section, we investigate the effect of defocusing the object, i.e., Γ is now

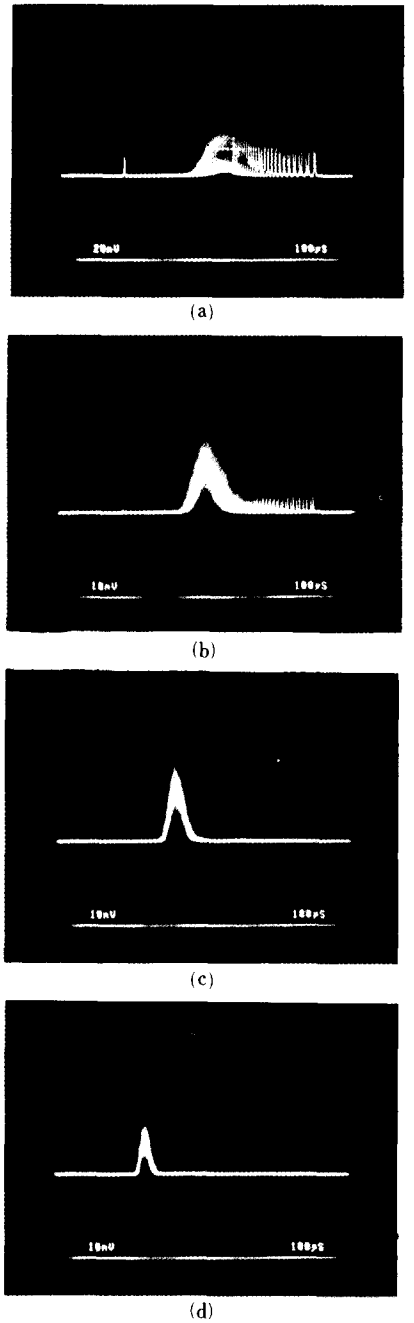

(a) (b) (c) (d)

Fig.5. MTF measurements in structural tuning:
(a) Δx=1.524*mm*; f_c = 3.95 lines/*mm* predicted, 3.8lines/*mm* measured,
(b) Δx =5.46*mm*; f_c = 5.46 lines/*mm* predicted, 5.3 lines/*mm* measured,
(c) Δx=3.429*mm*; f_c = 8.88 lines/*mm*, predicted, 8.7lines/*mm* measured,
(d) Δx=5.510*mm*; f_c = 14.28 lines/*mm* predicted, 14.3lines/*mm* measured.

placed in an out-of-focus plane. If the object is moved a z-distance on the optical axis out of focus, the field distribution due to the pupil u(x) on the out-of-focus object plane may be approximated by the Fresnel diffraction and it can be written as

$$U(x') = \frac{\exp(jkz)}{j\lambda z}\int_{-\infty}^{\infty} U(x_0)\, e^{j\frac{k}{2z}(x_0 - x')^2}\, dx_0, \qquad (26)$$

where k is the wave number, given by $2\pi/\lambda$, and $U(x_O)$ is the field distribution on the in-focus plane. Expressing U(x′) in terms of the pupil function u(x),

$$U(x') = \frac{-\exp(jkz)\exp(j_2^k \pi x'^2)}{\lambda^2 f_t z}$$

$$\iint_{-\infty}^{\infty} u(x)\, e^{-j\frac{2\pi}{\lambda f_t} x x_0} e^{j\frac{k}{2z} x_0^2} e^{-j\frac{k}{2} x_0 x'}\, dx dx_0. \qquad (27)$$

The distribution V(x′) on the out-of-focus plane, originated from the other pupil v(x), can be found in the same way. Replacing U(x) and V(x) with U(x′) and V(x′), respectively, in Eq. (17) yields

$$OTF(f_x, z) = \exp(j\pi\lambda z f_x^2)$$

$$\int_{-\infty}^{\infty} u(x)\, v^*(x - \lambda f_t f_x)\, e^{-j\frac{2\pi}{f_t} f_x z x} dx. \qquad (28)$$

The Fresnel approximation in Eq. (26) is valid under the two conditions, known as the Fresnel conditions[3]. Such conditions require limited bounds on the relative size of both the input and the output planes, and the distance z. For Eq. (28) to be accurate, the range of defocusing distance z must be constrained by the Fresenl conditions.

The defocused system is now analyzed for the particular case of the clear pupil functions. Substituting the clear pupil functions u(x) with an offset distance Δx and v(x) into Eq. (28), we find

$$OTF(f_x, z) = e^{-j\frac{\pi}{f_t}\Delta x f_x z}\,|OTF|, \qquad (29)$$

where |OTF| is the modulation transfer function (MTF) given by

$$MTF(f_x, z) = K\exp\{-\frac{\alpha}{2}(f_x - \frac{\beta}{\alpha})^2\}, \qquad (30)$$

with

$$\alpha = (\frac{\pi W_0 z}{f_t})^2 + (\frac{\lambda f_t}{W_0})^2, \quad \beta = \frac{\lambda f_t \Delta x}{W_0^2},$$

and

$$K = \exp[\frac{1}{2}\{(\frac{\beta^2}{\alpha}) - (\frac{\Delta x}{W_0})^2\}].$$

The parameter K contributes to the OTF as an amplitude control factor. The profile of the MTF is generally Gaussian with respect to f_x, but depends explicitly on the other parameters, in contrast with the in-focus case. A variety of MTFs can be obtained by varying the parameters Δx, W, and f.

The MTF of this system was estimated experimentally by scanning a frequency-varying grating placed in various out-of-focus planes. Traces of the MTF for various defocusing distances are shown in Fig.6, where the fixed values for the parameters are Δx=2.7 mm, W_O=1.0 mm, f_1= 610 mm, and λ=632.8 nm. In the experiments, the defocusing distances z was increased gradually, and the MTF curves were measured on the oscilloscope. Fig.6 (a)-(d) are the pictures of the displayed MTF response. They must be compared to Fig.7 which is plotted using the same parameters based on Eq. (30). In Fig.7, each case of the experiments in Fig.6 is represented by a line denoting a specific value of z. The measurements are in agreement with the predictions, in that as the defocusing distance increases, the frequency corresponding to the MTF peak moves from the high frequency range to the low frequency range, and the magnitude of the peak decreases. The parameters determining the MTF characteristics are the defocusing distance z, the size of the pupil function W, the offset distance Δx, the focal length f, and the wavelength λ. Therefore, recognizing the role of each parameter, the control of one or a combination of parameters provides versatile OTF tunability. An additional application of the dependence of the OTF characteristics on the defocusing parameter z is space variant filtering, which can be effected by tilting the object with respect to the optical axis so that different parts of the objects are at different defocusing distances.

IV. Conclusion

A practical type of incoherent optical pro-

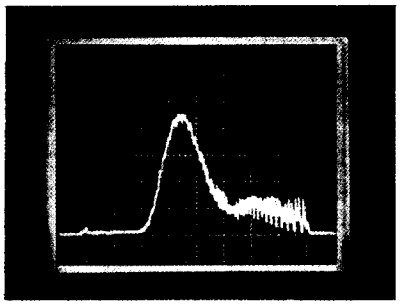

(a)

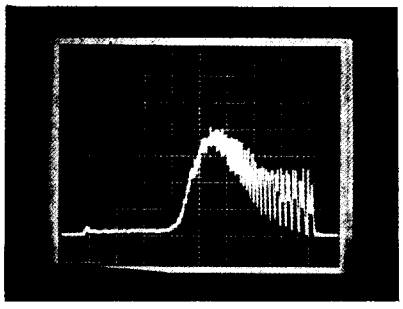

(b)

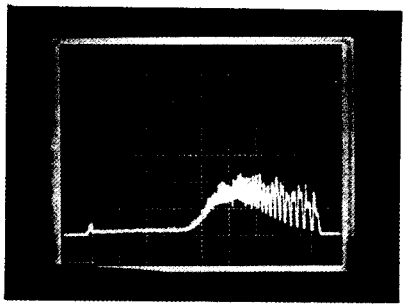

(c)

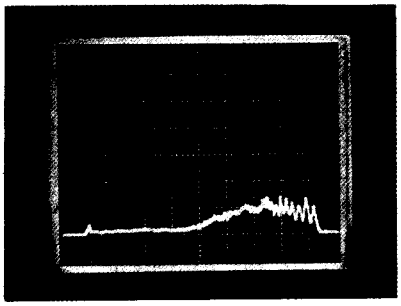

(d)

Fig.6. MTF measurements with $\Delta x=2.7\ mm$ in defocused object tuning: (a) $z=0\ mm$ (in focus), $f_c=7.0$ lines/mm measured, (b) $z=50\ mm$, $f_c=4.3$ lines/mm measued, (c) $z=120\ mm$, $f_c=2.8$ lines/mm measured, (d) $z=170\ mm$, very low f_c measured.

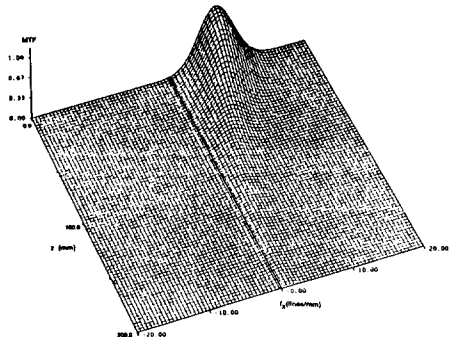

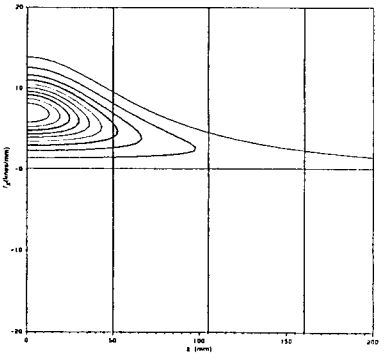

Fig.7. MTF plot in defocused object tuning from calculation using the same values of parameters as for the experiment Fig. 6.

cessing system exploiting an AOM for heterodying and an optical scanner as a spatial processing element is presented and analyzed in depth, as compared with a conventional incoherent processor and a bipolar two-pupil system.

The system's OTF can be written as the cross-correlation of the two pupil functions used in the systems. Since the OTF and the PSF of the system are wavelength-dependent, a tolerable range of the spectral width of the light source was examined to achieve an accurate spatial filtering operation. Considered is also the bandwidth requirement as an information processor, depending upon the system specifications given.

Two techniques for tuning the OTF of the system were proposed and verified in the MTF measurements; structural tuning and defocused object tuning. The structural tuning method is easy to implement but only applicable to 1-D operations. A controllable system parameter,

which is an out-of-focus distance, is added for the defocused object tuning method. Analaysis and the measurements showed that as the defocusing distance increases, the OTF gradually shows the lowpass filtering characteristics. The effects of varying the other parameters in the method were also investigated. The unique advantages of the incoherent system in this paper is that most of the complexity of the system is confined in the pupil generating part of the setup and much more flexibility can exist in designing the light receiving and detecting part. As a consequence, the requirements of the receiving optics are relaxed and the setup is adaptible to the objects of different sizes.

The applications of the system remains open for futher research, such as the application of the real time optical signal/image processing, robot vision, remote sensing, etc. The enhnacement of the system may in addition be made by adopting the features of multi-pupil and multi-channel PSF synthesis and the spatial carrier modulation.

References

[1] J.T. Tippett, D.A. Berkowitz, L.C. Clapp, C.J. Koester and A. Vanderburgh, Jr., Optical and electro-optical information processing, MIT press, Massachusetts, 1965.

[2] R.L. Stermer, Optical Information Processing for Aerospace Applications II, Proc. NASA conference, Publication 2302, Langley Research Center, Hampton, Virginia, 1983.

[3] J.W. Goodman, Introduction to Fourier Optics, McGraw-Hill, New York, 1968.

[4] G.L. Rogers, Noncoherent Optical Processing, Wiley, New York, 1977.

[5] W.T. Rhodes and A.A. Sawchuk, "Incoherent Opitcal Processing," in Optical Information Processing: Fundmentals, S.H. Lee, ed. (Topics in Applied Physics vol. 48) Springer-Verlag, New York, 1981

[6] S. Lowenthal and P. Chavel, "Noise problem in optical image processing," in Applications of Holography and optical Data Processing, E. Marom, A.A. Friesem and E. wiener-Avnear, Eds. Pergamon Press, New York, pp. 45-55, 1977.

[7] A.W. Lohmann and W.T. Rhodes, "Two-pupil synthesis of optical transfer functions," Appl. Opt., vol. 17, pp. 1141-1151, 1978.

[8] T.C. Poon and A. Korpel, "Optical transfer function of an acousto-optic heterodyning image processor," Appl. Opt., vol. 4, pp. 317-319, 1979.

[9] A. Papoulis, Signal Analysis, McGraw-Hill, New York, 1977.

[10] Hughes Series 3000 Laser Systems, Hughes Aircraft Company Carlsbad, California

著 者 紹 介

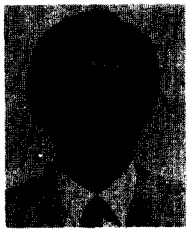

朴 鎭 雨 (正會員)

1955年 7月 5日生. 1979年 2月 고려대학교 전자공학과 졸업. 1980年 한국통신기술연구소 연구원. 1983年 8月 Clemson University 공학석사 학위 취득, 1987年 11月 Virginia 공대 공학박사 학위 취득. 1988年 3月 ~명지대학교 전자공학과 재직. 1989年 3月 ~ 현재 고려대학교 전자전산공학과 재직중. 주관심분야는 광섬유통신, 광신호 및 영상처리, 디지탈 영상 신호처리 등임.